

Kinetic Characterization of Hypophosphatasia Mutations With Physiological Substrates

SONIA DI MAURO,^{1,2} THOMAS MANES,¹ LOVISA HESSLE,^{1,3} ALEXEY KOZLENKOV,³
JOÃO MARTINS PIZAURU JR.,² MARC F. HOYLAERTS,⁴ and JOSÉ LUIS MILLÁN¹

ABSTRACT

We have analyzed 16 missense mutations of the tissue-nonspecific AP (TNAP) gene found in patients with hypophosphatasia. These mutations span the phenotypic spectrum of the disease, from the lethal perinatal/infantile forms to the less severe adult and odontohypophosphatasia. Site-directed mutagenesis was used to introduce a sequence tag into the TNAP cDNA and eliminate the glycosylphosphatidylinositol (GPI)-anchor recognition sequence to produce a secreted epitope-tagged TNAP (*set*TNAP). The properties of GPI-anchored TNAP (*gpi*TNAP) and *set*TNAP were found comparable. After introducing each single hypophosphatasia mutation, the *set*TNAP and mutant TNAP cDNAs were expressed in COS-1 cells and the recombinant flagged enzymes were affinity purified. We characterized the kinetic behavior, inhibition, and heat stability properties of each mutant using the artificial substrate *p*-nitrophenylphosphate (pNPP) at pH 9.8. We also determined the ability of the mutants to metabolize two natural substrates of TNAP, that is, pyridoxal-5'-phosphate (PLP) and inorganic pyrophosphate (PPi), at physiological pH. Six of the mutant enzymes were completely devoid of catalytic activity (R54C, R54P, A94T, R206W, G317D, and V365I), and 10 others (A16V, A115V, A160T, A162T, E174K, E174G, D277A, E281K, D361V, and G439R) showed various levels of residual activity. The A160T substitution was found to decrease the catalytic efficiency of the mutant enzyme toward pNPP to retain normal activity toward PPi and to display increased activity toward PLP. The A162T substitution caused a considerable reduction in the pNPPase, PPiase, and PLPase activities of the mutant enzyme. The D277A mutant was found to maintain high catalytic efficiency toward pNPP as substrate but not against PLP or PPi. Three mutations (E174G, E174K, and E281K) were found to retain normal or slightly subnormal catalytic efficiency toward pNPP and PPi but not against PLP. Because abnormalities in PLP metabolism have been shown to cause epileptic seizures in mice null for the TNAP gene, these kinetic data help explain the variable expressivity of epileptic seizures in hypophosphatasia patients. (J Bone Miner Res 2002;17:1383–1391)

Key words: genetic disease, missense mutations, catalytic efficiency, natural substrates, alkaline phosphatase

INTRODUCTION

Alkaline phosphatase (orthophosphoric-monoester phosphohydrolase, alkaline optimum EC 3.1.3.1) is present in most species from bacteria to man.⁽¹⁾ The enzyme was discovered by

Robison⁽²⁾ within ossifying bone and cartilage and he proposed that this catalytic action had a role in hydrolyzing monophosphate esters thus increasing the concentration of inorganic phosphate. The clearest evidence that APs are important in bone mineralization has been provided by studies of human hypophosphatasia where a deficiency in the tissue-nonspecific AP (TNAP) isozyme is associated

The authors have no conflict of interest.

¹The Burnham Institute, La Jolla, California, USA.

²Faculdade de Ciências Agrárias e Veterinárias/UNESP, Jaboticabal, São Paulo, Brazil.

³Center for Molecular and Vascular Biology, University of Leuven, Leuven, Belgium.

⁴Department of Medical Genetics, Umeå University, Umeå, Sweden.

with defective bone mineralization.⁽³⁾ The clinical severity in hypophosphatasia patients varies widely.⁽⁴⁾ The different syndromes, listed from the most severe to the mildest, are perinatal, infantile, childhood, adult, and odonto- and pseudohypophosphatasia. The phenotypic abnormalities range from complete absence of bone mineralization and stillbirth to spontaneous fractures and loss of deciduous teeth in adult life. The severe forms of hypophosphatasia usually are inherited as autosomal recessive traits with parents of such patients showing subnormal levels of serum AP activity. Variable expressivity and incomplete penetrance are common features.⁽⁴⁾ For the milder forms, that is, adult and odontohypophosphatasia, an autosomal dominant pattern of inheritance has been documented.⁽⁴⁾ The molecular basis for these complex patterns of inheritance is not understood completely.

The first identified hypophosphatasia mutation was a missense mutation in exon 6, A162T.⁽⁵⁾ Subsequently, compound heterozygosity and new mutations, (i.e., R54C, R54P, E174K, Q190P, Y246H, D277A, D361V, and Y419H) were reported.^(6,7) Other mutations found since include G317D⁽⁸⁾; F310L and G439R⁽⁹⁾; E281K, A160T, and a frame shift mutation at position 328 and another at position 503.⁽¹⁰⁾ Mornet et al.⁽¹¹⁾ reported 16 new missense mutations in European patients (i.e., S-1F, A23V, R58S, G103R, G112R, N153D, R167W, R206W, W253X, E274K, S428P, R433C, G456S, G474R and two splice mutations in intron 6 and 9, respectively). Interestingly, in a recent historical vignette, the mutations present in the original hypophosphatasia patient studied by Rathbun in 1948,⁽³⁾ were identified also.⁽¹²⁾ That 3-week-old boy was a compound heterozygote for the A97T and D277A mutations.

To date, a total of 65 distinct mutations have been described for the human TNAP gene.⁽¹³⁾ Mutagenesis studies and structural predictions^(14,15) have increased our understanding of the correlation between genotype and phenotype. Interestingly, defective trafficking of several hypophosphatasia mutations (i.e., R54C,⁽¹⁶⁾ A162T,⁽¹⁷⁾ and G317D⁽¹⁸⁾) through the Golgi has been established as a mechanism that contributes to the variable expressivity of this disease.

In this report we provide a kinetic characterization of 16 different hypophosphatasia mutations that span the spectrum of severity of the disease. The mutant enzymes were produced in a soluble secreted form to enable us to characterize their kinetic properties independently of how efficiently these mutant enzymes may be exported to the cell membrane. This strategy also allowed us to increase the yield of purified recombinant TNAP and obtain the quantities necessary to perform the kinetic studies using physiological substrates at neutral pH. We have characterized these mutants for their hydrolyzing and transferase activity using the synthetic substrate *p*-nitrophenylphosphate (pNPP) and the two natural TNAP substrates (i.e., pyridoxal-5'-phosphate [PLP] and inorganic pyrophosphate [PPi]) that are associated with the clinical manifestations of the disease.⁽⁴⁾ Our data indicate that the preferential use of PPi versus PLP as substrate by some missense mutations can help explain the variable expressivity of the epileptic sei-

zures and apnea, which are prominent in some cases of hypophosphatasia.

MATERIALS AND METHODS

Wild-type and TNAP mutant cDNAs

The TNAP cDNA (ATCC no. 59635; American Type Culture Collection, Manassas, VA, USA) was used as template for the construction of the wild-type and mutated TNAP expression vectors. To facilitate isolation of the recombinant enzymes, an FLAG epitope (5'-TTA CTT GTC ATC GTC GTC CTT GTA GTC-3') was introduced after the Leu489, followed by a termination codon to eliminate the glycosylphosphatidylinositol anchoring signal. This secreted epitope-tagged TNAP (*sef*TNAP) was used as a template for the introduction of all hypophosphatasia mutations.

Site-directed mutagenesis was performed as described by Tomic.⁽¹⁹⁾ The sequence of the primers used to generate the mutations are shown in the following with amino acid changes underlined: A16V, G TAC TGG CGA GAC CAA GTC CAA GAG ACA CTG; R54C_c, CC AGG GTT GTG GTG GAG CTG ACC CTT GAG GAT GCA GGC AGC CGT C; R54P_c, CC AGG GTT GTG GTG GAG CTG ACC CTT GAG GAT GGG GGC AGC CGT C; A94T_c, G CTC TCC GGT GGC GGT GCC GGT ACT GTC AGG G; A115V_c, CGT CTC ACG CTC AGT GGC TAC GCT TAC CCC CAC; A160T_c, CG TCT CTC AGC CGA GTG GGC GTA GGT GGC GCT GG; A162T_c, CG TCT CTC AGC CGA GTG GGT GTA GGC GGC; E174K_c, CG TCT CAA GGC CTC AGG GGC CAT CTT GTT GTC TGA G; E174G_c, CG TCT CAA GGC CTC AGG GGC CAT CCC GTT GTC TGA G; R206W, ATT GAC GTG ATC ATG GGG GGT GGC TGG AAA TAC ATG T; D277A_c, CG TCT CTA CTG CAT GGC CCC CGG CTC G; E281K, C GTC TCG CAG TAC AAG CTG AAC AGG AAC AA; G317D_c, C GTC TCG CCC GTG GTC AAT TCT GTC TCC TTC CAC C; D361V, CG TCT CTC ACT GCG GTC CAT TCC CAC GTC; V365I, CG TCT CTC ACT GCG GAC CAT TCC CAC ATC TTC ACA TTT GG; G439R_c, AT GGG GCC CTT GGA GAA GAC GGC CAC GTC CTC CCG GCC GTG GGT C.

All TNAP cDNAs were subcloned into the pcDNA 3.1 expression vector (*HindIII/SpeI*) downstream from the SV40 early promoter. All constructs were verified by restriction digestion and DNA sequencing.

Homology modeling of the TNAP molecule

We used the program MODELLER⁽²⁰⁾ to construct a homology model of dimeric TNAP based on a recently published structure of human placental AP (PLAP).⁽²¹⁾ The relatively high level of sequence similarity (55% identical residues) between amino acid sequences of TNAP and PLAP simplified the task of preparing the initial alignment. Five different models of TNAP were produced and the one with the lowest MODELLER objective function was used for further examination. Metals and phosphate ions were included during the calculation to preserve the geometry of

their conserved ligands. The only areas where the models differed significantly were a three-amino acid insertion after Ser241 and the C-terminal fragment after Ser485, for which no template in the structure of PLAP was available.

Tissue culture and enzyme purification

The expression constructs were transfected into COS-1 cells by the diethylaminoethyl (DEAE) dextran (100 mg/ml in Tris-buffered saline [TBS]) procedure and a 10% DMSO/2% fetal calf serum shock to increase the transfection efficiency. The medium (25 ml/150-mm plate) was collected 72, 120, and 168 h after transfection. Each secreted FLAG-tagged mutant enzyme was purified using an anti-FLAG M2 monoclonal antibody affinity column (Sigma, St. Louis, MO, USA) as per the manufacturer's instructions. GPI-anchored wild-type and mutant enzymes were extracted 72 h after transfections using a 1:1 mixture of *n*-butanol and 50 mM of sodium acetate buffer, pH 5.5, containing 100 mM of NaCl, 20 μ M of ZnCl₂, 2 mM of MgCl₂, and 0.5% thimerosal.

Kinetic measurements

For the kinetic studies, the affinity-purified enzymes were diluted in TBS to the same optical density at 280 nm. Enzymatic reactions were carried out using pNPP in 1 M of diethanolamine (DEA) buffer (pH 9.8) containing 1 mM of MgCl₂ and 20 μ M of ZnCl₂. Enzyme reactions also were performed at pH 7.5 in 50 mM of Tris buffer, containing 1 mM of MgCl₂ and 20 μ M of ZnCl₂. The inhibition properties of the mutant enzymes toward L-homoarginine and levamisole were measured in microtiter plates by adding 2 μ l of enzyme to a mixture of 100 μ l of 10 mM of pNPP in DEA, pH 9.8, supplemented with 1 mM of MgCl₂, 20 μ M of ZnCl₂, and 100 μ l of inhibitor solution (ranging in concentration from 0 to 10 mM for L-homoarginine and 0 to 100 μ M for levamisole). For heat stability studies, the GPI-anchored TNAP and all *sef*TNAP mutants were diluted in TBS containing 10% casein, 1 mM of MgCl₂, and 20 μ M of ZnCl₂ and incubated in a thermocycler for 10 minutes at a temperature ranging from 45 to 62.5°C at 2.5°C intervals as previously described.⁽²²⁾ Heat stability was determined also by inactivation at 56°C up to 25 minutes. Ten-microliter samples were removed every 5 minutes and pipetted into a well of a microtiter plate kept on ice. Residual activities then were measured in triplicate. Michaelis-Menten constants (K_m and V_{max}) were determined graphically from Woolf plots.

PLP and pyrophosphatase activity

PLP and pyrophosphatase activities were assayed discontinuously at 37°C. Standard assay conditions were 50 mM of Tris buffer, pH 7.5, containing 1 mM of MgCl₂ and 20 μ M of ZnCl₂ and increasing concentrations of substrate (0.1 μ M–10 mM) in a final volume of 0.08 ml. The reaction was initiated by the addition of the enzyme and interrupted with the addition of 0.02 ml of 50% trichloroacetic acid at appropriate times as described.⁽²³⁾ Inorganic phosphate re-

leased in the reaction medium was determined by the procedure of Heinonen and Lahti.⁽²⁴⁾ All determinations were carried out in duplicate and the initial velocities were constant for at least 60 minutes provided that <5% of substrate was hydrolyzed. Controls without added enzyme were included in each experiment to measure the nonenzymatic hydrolysis of the substrate. Comparisons between mean values were done using the Tukey test at 5% probability level.

Protein determination and Western blots

The enzyme concentration of each purified sample was determined by the Quantigold (Diversified Biotech, Boston, MA, USA) kit using bovine serum albumin (BSA) as a standard and independently by a densitometric analysis of Western blots. For Western blots, electrophoresed proteins were transferred to polyvinylidene difluoride (PVDF) membranes (Amersham Pharmacia Biotech, Buckinghamshire, UK) followed by blocking in 25 mM of Tris-HCl, pH 7.4, containing 137 mM of NaCl (TBS) also containing 1% Tween 20 and 2% BSA. Subsequently, the membranes were incubated with 1 μ g/ml of M2 anti-FLAG antibody (Sigma) in TBS for 60 minutes. After three washes in TBS, the membranes were treated with a second antibody using the Vectastain ABC kit (Vector Laboratories, Burlingame, CA, USA) following the manufacturer's instructions.

RESULTS

Hypophosphatasia mutations

We introduced an eight-amino acid FLAG tag sequence and a premature stop codon at position 489 into the wild-type TNAP cDNA to facilitate the expression, recovery, and purification of the large amounts of recombinant enzyme from COS-1 cells needed for the subsequent characterizations. To ascertain how these modifications might affect the properties of the resulting enzyme, we compared the *sef*TNAP and the wild-type GPI-anchored TNAP (*gpi*TNAP) in terms of affinity for substrate, inhibition properties, and heat stability. We observed a small, but statistically significant increase in K_m for *sef*TNAP (0.45 ± 0.04 mM) compared with *gpi*TNAP (0.34 ± 0.10 mM; $p < 0.05$) while the inhibition constants toward the uncompetitive inhibitor L-homoarginine (3.6 mM vs. 4.0 mM) were comparable. Both *sef*TNAP and *gpi*TNAP showed 50% inactivation at 56°C. The *sef*TNAP showed a 15-minute half-life compared with a 13-minute half-life for *gpi*TNAP when subjected to a time-dependent inactivation at 56°C.

Using *sef*TNAP as a template, we constructed 16 TNAP mutant cDNAs corresponding to a wide spectrum of reported hypophosphatasia mutations (Table 1) and expressed them in COS-1 cells. All mutant cDNAs were expressed in the cells and recombinant protein could be recovered from the culture medium as shown by Western blot analysis (Fig. 1). The small differences in electrophoretic migration of the mutant TNAPs are reduced, but not eliminated, by neuraminidase treatment. The mutant enzymes were affinity-purified and characterized. The purified TNAPs also were

TABLE 1. HYPOPHOSPHATASIA MUTATIONS STUDIED

Mutations	Type	Inheritance	Compound heterozygote with	Reference
A16V	P/I	R	Y419H	Henthorn et al. ⁽⁷⁾
R54C	P/I	R	D277A	Henthorn et al. ⁽⁷⁾
R54P	P/I	R	Q190P	Henthorn et al. ⁽⁷⁾
A94T	Odonto	D	none	Goseki-Sone et al. ⁽²⁹⁾
A115V	Adult	D	none	Watanabe et al. ⁽²⁸⁾
A160T	Adult	R	F310L	Goseki-Sone et al. ⁽²⁹⁾
A162T	P/I	R	none	Weiss et al. ⁽⁵⁾
E174K	I/Adult	R?	D361V/D277A/E274K	Henthorn et al. ⁽⁷⁾
E174G	Odonto	D?	503-fr. Shift	Goseki-Sone et al. ⁽²⁹⁾
R206W	Lethal	D?	None	Mornet et al. ⁽¹¹⁾
D277A	I/Adult	R	R54C/E174K	Henthorn et al. ⁽⁷⁾
E281K	P/I	R	503-fr. Shift	Orimo et al. ⁽¹⁰⁾
G317D	Lethal	R	none	Greenberg et al. ⁽⁸⁾
D361V	Adult/Odonto	D?	E174K	Henthorn et al. ⁽⁷⁾
V365I	I	R	F310L	Goseki-Sone et al. ⁽²⁹⁾
G439R	P/I	R	F310L	Ozono et al. ⁽⁹⁾

Included are the type of hypophosphatasia in which the mutation was found, the mode of inheritance, with what other mutation it was found in compound heterozygotes (if applicable), and the original reference that identified the mutation.

P, perinatal hypophosphatasia; I, infantile hypophosphatasia; Odonto, odontohypophosphatasia; Adult, adult hypophosphatasia; R, recessive inheritance; D, dominant inheritance.

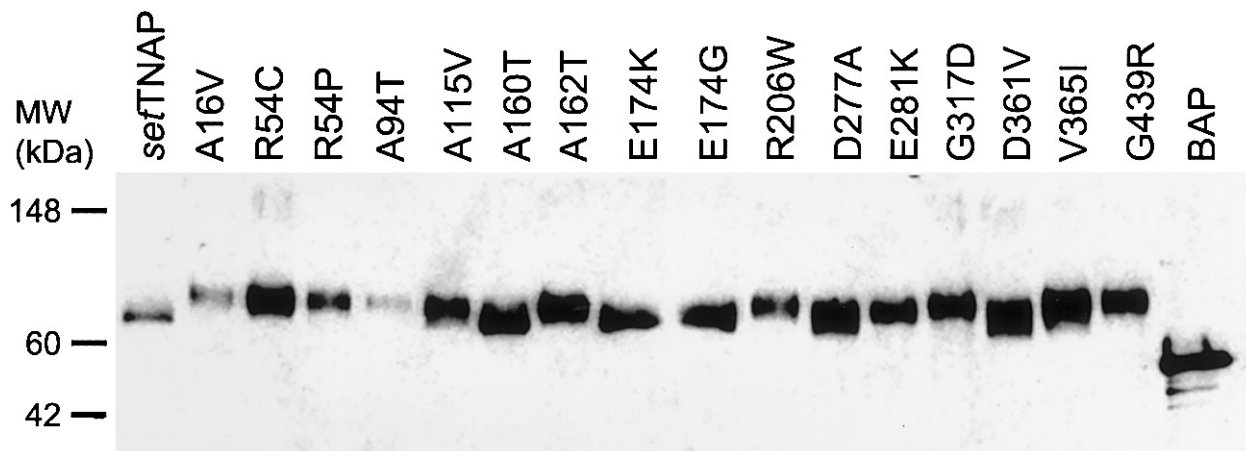


FIG. 1. Western blot analysis of the *sefTNAP* and secreted hypophosphatasia mutant enzymes. All mutant enzymes were expressed and secreted appropriately into the culture medium. The *sefTNAP* and a commercial secreted and flagged-bacterial AP (BAP) were used as positive controls.

electrophoresed on nondenaturing gels and stained by Coomassie blue as well as for AP activity (not shown). This analysis revealed that although all mutant enzymes were isolated from the medium as dimers, only some mutants retained catalytic activity. In fact, six mutant TNAPs were completely inactive (i.e., R54C, R54P, A94T, R206W, G317R, and V365I). However, 10 of the 16 mutants displayed various amounts of residual activity (i.e., A16V, A115V, A160T, A162T, E174K, E174G, D277A, E281K, D361V, and G439R). Figure 2 shows a model representation of those amino acid substitutions that lead to complete inactivation of the TNAP activity, as well as of those mutations that result in mutants with residual enzyme activity. The model of TNAP was constructed based on the crystal structure of human PLAP.⁽²¹⁾

Kinetic parameters under optimal *in vitro* conditions

Table 2 shows the kinetic parameters and heat stability properties of the 10 active mutant TNAPs using the artificial substrate pNPP at pH 9.8. The k_{cat} value for the wild-type *sefTNAP* was 551. The mutations introduced major changes in affinity for the substrate as well as in the catalytic rate constants.

The K_m values for the D277A, D361V, and G439R mutants were increased 2.2-, 344-, and 253-fold compared with *sefTNAP*; the E281K mutant on the contrary showed a 50% reduction in K_m , reflecting a higher affinity for pNPP. The A16V and A115V mutations result in reduced K_m values in association with a reduction in k_{cat} , yielding a catalytic efficiency of 10% of the control value. The D361V and

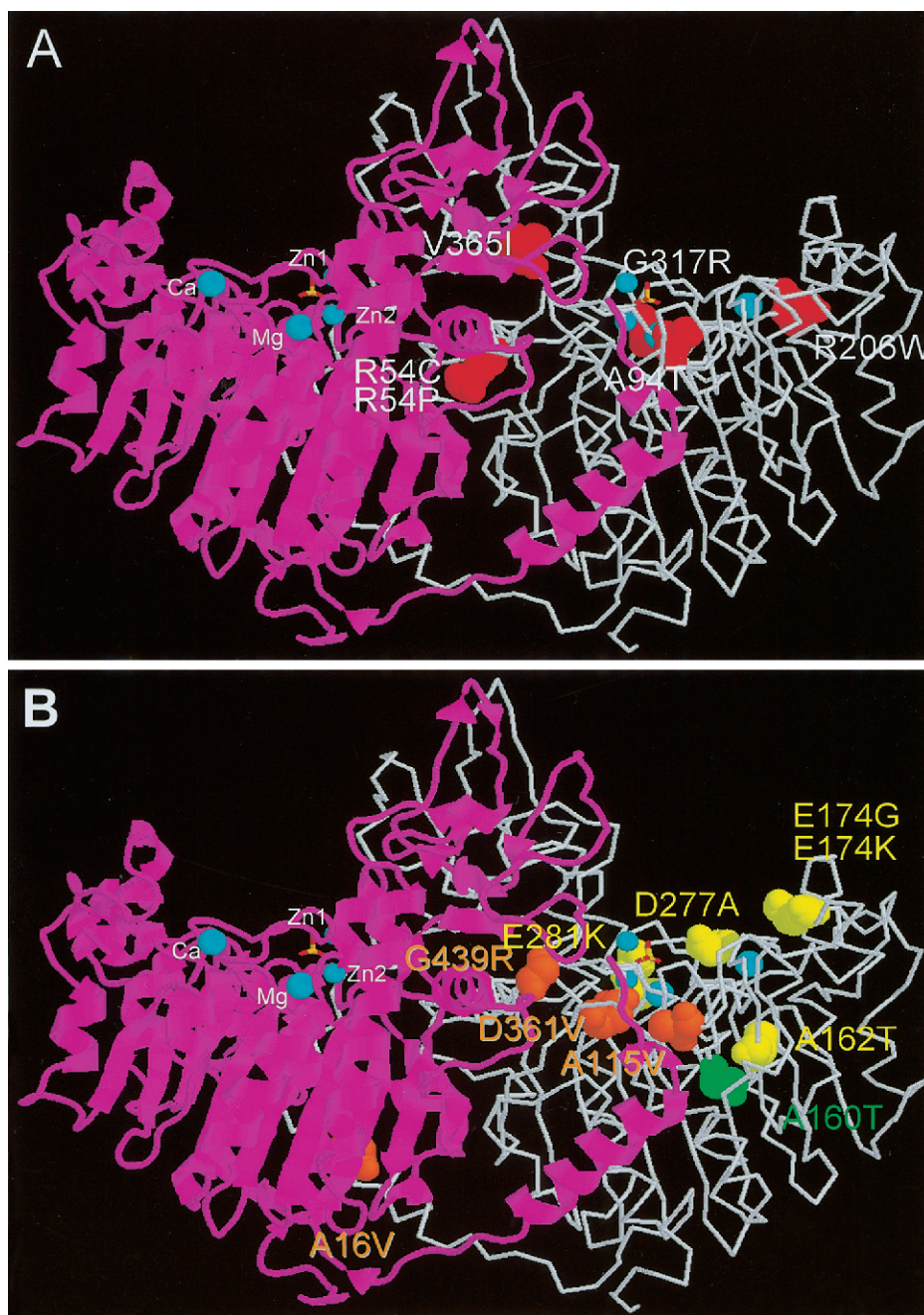


FIG. 2. Location of the investigated hypophosphatasia mutants on the modeled three-dimensional structure of TNAP. (A) Amino acid substitutions leading to complete loss of function (R54C, R54P, A94T, R206W, G317R, and V365I) are shown in space-filling representation colored in red. Amino acid substitutions leading to various degrees of TNAP activity loss are represented as space-filling residues with different colors: orange, very low activity remaining (A115T, D361V, and G439R); yellow, moderate activity remaining (E174G, E174K, D277A, and E281K); and green, activity comparable or greater than with wild-type TNAP (A160T). The mutations are shown as space-filling residues only on the panel A subunit, which is displayed in backbone representation and colored in white. The panel B subunit is displayed as ribbons emphasizing regions of secondary structure and is colored in magenta. The metal ions (Zn1, Zn2, Mg, and Ca) are identified in the panel B subunit for reference.

G439R mutants had the highest K_m with the lowest k_{cat} values and consequently had the lowest catalytic efficiency. The change of a glutamic acid to glycine or lysine in E174K and E174G had little impact on K_m and k_{cat} , despite the major change of charge in the E174 mutant. The catalytic efficiency decreased to 50% for the E174G mutant. The A160T and A162T mutants had the same value for K_m , but A160T showed an increase of 100% in k_{cat} , resulting in an enzyme with an almost threefold increased catalytic efficiency compared with *ser*TNAP.

TNAP loses its activity very rapidly at 56°C.⁽²⁵⁾ As shown in Table 2, most mutations had very little impact on

the stability of the mutants. Because D361V and G439R mutants had very low activity, they could not be tested in the heat stability studies. The enzyme resulting from the D277A substitution at 56°C loses activity with a half-life of 5 minutes. Both D277A, a mutation present in infantile and adult hypophosphatasia, and A16V, present in perinatal and infantile hypophosphatasia, progressively lost their activity above 47.5°C; at 57.5°C the D277A mutant was almost inactive after 15 minutes and the A16V mutant retained 20% of its initial activity. Interestingly, whereas the E174G mutant had a heat stability comparable with that of *ser*TNAP, the E174K mutant appeared to be more stable

TABLE 2. KINETIC PARAMETERS AND STABILITY PROPERTIES OF *set*TNAP AND HYPOPHOSPHATASIA MUTATIONS

MUTANT	K_m (mM)	Half-life 56°C (min)	50% Inactivation (°C)	L-homoarginine K_i (mM)	Levamisole K_i (μ M)	k_{cat} (s^{-1})	$k_{cat}/K_m \times 10^3$ ($M^{-1}s^{-1}$)
<i>set</i> TNAP	0.45 ± .04	15.0	56.0	4.0	51.0	551	1224
A16V	0.34 ± .07	12.2	55.0	4.8	ND	40	116
A115V	0.32 ± .04	12.8	55.0	5.6	ND	36	114
A160T	0.34 ± .04	12.2	56.0	3.8	55.0	1083	3187
A162T	0.34 ± .06	12.0	55.5	5.6	30.0	331	973
E174G	0.47 ± .07	13.0	55.5	3.0	68.0	294	627
E174K	0.34 ± .07	>25.0	57.0	4.3	100.0	452	1329
D277A	1.0 ± .09	5.0	53.0	6.0	64.0	350	350
E281K	0.24 ± .07	20.0	56.0	3.8	61.0	156	650
D361V	>155 ± 23	ND	ND	ND	ND	8	<0.05
G439R	114 ± 12	ND	ND	ND	ND	6	0.05

Measurements were done at pH 9.8 using pNPP as substrate.

(Table 2). After 15 minutes at 56°C (half-life for *set*TNAP) the E174K mutant retained 75% of its activity, making it the most stable enzyme tested. Also, the E281K mutant appeared to have gained stability with respect to *set*TNAP, with a half-life of 20 minutes.

The *set*TNAP and all active mutant enzymes were tested for their residual activity in the presence of the uncompetitive inhibitors L-levamisole or L-homoarginine. As shown on Table 2, the K_i value was only mildly affected for most mutated enzymes studied, using either inhibitor. The largest variation, a twofold increase in K_i for levamisole, was observed with the E174K mutant. Thus, the amino acid substitutions interfered less with enzyme inhibition than with the actual catalytic process.

PLP and pyrophosphatase activity at physiological pH

To validate whether the shift in activity measured for the TNAP mutants under optimal conditions (i.e., in the presence of a transphosphorylating alcohol at pH 9.8) reflects residual activities at more physiological pH, activity measurements were done at pH 7.5. As shown in Table 3, the relative activities of those six mutants that had retained sufficiently high activity at pH 9.8 were differentially affected at pH 7.5.

When measured with pNPP, the lowest k_{cat} was found in the case of the E174K mutation and the highest K_m was found for the A160T mutation. To further know whether the mutants would be active with physiological substrates, specific activity measurements also were done with two natural substrates (PPi and PLP) and their K_m and k_{cat} and catalytic efficiency were determined as reported in Table 3. In comparison with *set*TNAP, the K_m value with PPi and PLP was altered for all the mutant enzymes tested. When measured with PPi, the A162T and D277A mutants showed a considerable drop in K_m , indicative of facilitated substrate interactions. However, both mutants showed a strong reduction in k_{cat} , that is, leading to weak catalytic efficiencies. When PLP was the substrate, the mutants E174K and E281K showed the largest drop in k_{cat} (Table 3). The A160T mutation maintained a comparable catalytic efficiency by

simultaneously causing a raise in k_{cat} and K_m . For A162T and D277A we were not able, using this methodology, to detect any activity when PLP was the substrate. In contrast, *set*TNAP showed comparable catalytic efficiency for both PPi and PLP as substrates.

DISCUSSION

TNAP dysfunction has been associated with hypophosphatase, a disease characterized by deficiency in bone mineralization.⁽⁴⁾ In this study we characterized 16 mutations found in patients with a different degree of severity of the disease. To be able to perform our analysis with purified enzyme, we tagged the 3'-terminal sequence of the TNAP encoding cDNA with FLAG in front of the stop codon and the sequence encoding the GPI anchor. This approach made it possible to produce the large amounts of recombinant TNAP needed for the kinetic experiments at physiological pH, where the requirements for recombinant enzyme increased 20- to 100-fold for most mutants. The kinetic parameters determined for released *set*TNAP and membrane-bound TNAP were comparable, indicating that this approach would not confound the kinetic properties of the mutant enzymes. This strategy also enabled us to characterize the behavior of some missense mutations known to traffic abnormally through the Golgi.

All mutant TNAP were produced efficiently and secreted into the medium where they were recovered and purified. The purified recombinant TNAPs displayed small differences in migration on SDS-PAGE, which are in part explained by differences in the sialic acid content, because neuraminidase treatment reduced some of the heterogeneity. However, conformational changes resulting from the point mutations also are likely to contribute to this differential migration. The recombinant TNAPs were subjected also to electrophoresis on nondenaturing gels. This analysis confirmed that all mutants were produced and secreted as dimeric molecules even when the point mutation resulted in the complete abolishment of enzymatic activity.

TABLE 3. KINETIC PARAMETERS OF *set*TNAP AND TNAP MUTANTS AT pH 7.5 USING PPI, PLP, and pNPP as Substrates

TNAP mutant	PPI			PLP			pNPP		
	K_m (mM)	k_{cat} (s^{-1})	$\frac{K_{cat}}{K_m} \times 10^{-6} M^{-1} s^{-1}$	K_m (mM)	k_{cat} (s^{-1})	$\frac{K_{cat}}{K_m} \times 10^{-6} M^{-1} s^{-1}$	K_m (mM)	k_{cat} (s^{-1})	$\frac{K_{cat}}{K_m} \times 10^{-6} M^{-1} s^{-1}$
<i>set</i> TNAP	0.48 ± .027	66.74 ± 4.64	0.14	0.13 ± .027	20.69 ± 1.32	0.16	0.009 ± .002	0.843 ± 63.04	0.09
A160T	0.34 ± .0008	57.16 ± .37	0.17	0.35 ± .004	42.99 ± 0.37	0.12	0.017 ± .003	0.436 ± 17.02	0.02
A162T	0.06 ± .008	3.52 ± .34	0.05	ND	ND		0.008 ± .0008	0.431 ± 5.38	0.05
E174G	0.4 ± .09	59.72 ± 2.57	0.15	0.04 ± .0006	1.48 ± .04	0.04	0.009 ± .002	1.20 ± 117.71	0.10
E174K	0.24 ± .00	23.18 ± 0.001	0.09	0.09 ± .001	5.39 ± 1.42	0.06	0.005 ± .0003	0.100 ± 29.63	0.02
D277A	0.17 ± .00	4.31 ± .00	0.03	ND	ND		0.004 ± .0002	0.914 ± 36.1	0.20
E281K	0.27 ± .02	54.8 ± 14.48	0.2	0.09 ± .004	3.48 ± 0.22	0.04	0.008 ± .0015	7.18 ± 112.09	0.90

K_m 's were measured in buffered substrate at pH 7.5 in the presence of 1 mM of $MgCl_2$ and 20 μM of $ZnCl_2$.

The six mutations that produced inactive enzymes were found in patients with perinatal and infantile forms of hypophosphatasia alone or in compound heterozygosity. R54C and R54P are mutations present in patients with the perinatal form of hypophosphatasia.⁽⁶⁾ R54C has been shown to remain trapped inside transfected cells.⁽¹⁶⁾ Our data using a soluble epitope-tagged mutant enzyme indicate that the lack of activity is not only caused by inappropriate trafficking but that this mutation effectively abolishes catalytic activity. The same is true for the G317D mutation.⁽¹⁸⁾ Figure 2 shows that three inactivating mutations (V365I, R54C, and R54P) are close to the enzyme dimer interface and it is possible that these mutations severely destabilize dimer formation. Two mutations (G317D and A94T) are positioned close to the active site residues that are involved directly in the Zn^{2+} and Mg^{2+} coordination.⁽²¹⁾ Surprisingly, the R206W mutations are distant from the active site pocket, while still capable of causing loss of activity. However, this residue is close to a fourth metal site, which as reported recently, may be occupied by calcium ions in TNAP.⁽¹⁵⁾ D361V and G439R are mutations located in the Zn^{2+} coordination site and were the least active mutants, that is, around 100-fold less active than *set*TNAP. D361V has been found in dominantly inherited hypophosphatasia and this mutation was shown to inhibit the activity of the product of the remaining wild-type allele.⁽²⁶⁾ Previously, we have shown that mammalian APs behave as allosteric enzymes and that the heterodimers display properties that are not the weighted average of the properties of the homodimers.⁽²⁷⁾ So the kinetic properties of the D361V mutant and the fact that it forms heterodimers can explain its role in causing dominantly inherited hypophosphatasia. The same explanation may hold true for the A115V mutation, which was reported as dominant and found in a patient with adult hypophosphatasia.⁽²⁸⁾

One mutant (A160T)⁽²⁹⁾ had an increased k_{cat} when measured with pNPP at pH 9.8 and with PLP, but not when measured with PPI and pNPP at pH 7.5. In fact, an increase in K_m was observed for both PLP and pNPP under these conditions. This mutation was found in a patient compound heterozygote with an F310L who had only mild symptoms of adult hypophosphatasia. The A162T⁽⁵⁾ mutation displayed normal catalytic properties under optimal pH and buffer conditions. This is in contrast with results from Weiss et al.,⁽⁵⁾ who reported complete inactivation when this mutant was expressed in NIH3T3 cells. However, Shibata et al.,⁽¹⁷⁾ who expressed A162T in COS-1 cells, found that most of the A162T enzyme remained inside the cells providing an explanation for the Weiss et al.⁽⁵⁾ report of complete inactivation. Our experimental approach, using *set* enzymes enabled us to bypass this intracellular trafficking block and obtain data that indicate that the active site of the A162T mutant is largely unaffected by this substitution using pNPP as substrate at pH 9.8. Nevertheless, the A162T mutation showed considerable reduction in enzyme activity, using PPI and PLP as substrates at physiological pH. So the combination of reduced activity at physiological pH and deficient transport explains the severity of this mutation, which has been found in cases of perinatal hypophosphatasia.

The E174K⁽⁶⁾ and E174G⁽²⁹⁾ mutations were detected in a patient with the infantile form of the disease and in cases of adult and odontohypophosphatasia in compound heterozygosity. Our results show a significantly reduced activity for E174K and E174G when tested with PLP. Mutation E281K⁽¹⁰⁾ was found in a patient with a severe form of hypophosphatasia. A substantial loss of activity was found at pH 7.5 for both PPi and PLP. This mutation was discovered in an infant girl that exhibited profound hypomineralization and respiratory distress and died at 5 months of age. Mutation D277A produces an unstable enzyme with low k_{cat} values for all substrates analyzed (Tables 2 and 3) but particularly undetectable activity toward PLP. D277A was found in different compound heterozygous patients.⁽⁶⁾ Recently, in an interesting historical vignette, Mumm et al.⁽¹²⁾ identified this mutation in the original hypophosphatasia case reported by Rathbun in 1948.⁽³⁾ This severely affected boy that appeared well at birth developed epileptic seizures and cried as though in pain. These symptoms (i.e., epileptic seizures, high-pitched vocalizations, and apnea) are a prominent feature of the mouse model of hypophosphatasia⁽³⁰⁾ and these manifestations have been attributed to abnormal PLP metabolism^(31,32) resulting from a TNAP inactivation. Thus, the inability of these mutant enzymes (E174G, D277A, and E281K) to hydrolyze PLP clearly correlates with the clinical presentation of the disease.

In conclusion, our results contribute to the understanding of the variable expressivity of hypophosphatasia by pointing to the preferential use of PPi versus PLP displayed by some mutations. Data obtained using mouse models of hypophosphatasia, indicate that abnormalities in PLP metabolism^(31,32) explain the epileptic seizures and apnea that are so prevalent in the TNAP knockout mice. However, the bone abnormalities are unrelated to the abnormal PLP metabolism but can instead be explained by the accumulation of PPi,⁽³³⁾ a potent inhibitor of mineralization. Hypophosphatasia patients⁽⁴⁾ and mice deficient in TNAP⁽³⁴⁾ excrete increased amounts of phosphoethanolamine in the urine. However, the metabolic pathway that leads to this phosphoethanolamine increase currently is unknown and no clinical abnormality has been correlated to this biochemical finding to date.

Patients that inherit mutations such as E174G, D277A, or E281K, which are very inefficient in hydrolyzing PLP, would be expected to manifest more severe seizures and apnea than patients with other mutations. Furthermore, these mutant enzymes often are found in compound heterozygous individuals in heterodimeric combination with other missense mutations. We know that heterodimers have catalytic properties that are not the pounded average of those of the corresponding homodimers because of the allosteric properties of mammalian APs.⁽²⁷⁾ Thus, preferential substrate use by each monomer in combination with heterodimer formation and even impaired intracellular trafficking are all mechanisms that help explain the complex variable expressivity often observed in hypophosphatasia.

ACKNOWLEDGMENTS

This work was supported by grants CA42595 and DE12889 from the National Institutes of Health (NIH; Be-

thesda, MD, USA). Sonia Di Mauro was supported by a fellowship from the Conselho Nacional de Desenvolvimento Científico e Tecnológico (CNPq), São Paulo, Brasil.

REFERENCES

- McComb RB, Bowers GN Jr, Posen S 1979 Alkaline Phosphatases, Plenum, New York, NY, USA.
- Robison R 1923 The possible significance of hexosephosphoric esters in ossification. *Biochem J* **17**:286–293.
- Rathbun JC 1948 Hypophosphatasia: A new developmental anomaly. *Am J Dis Child* **75**:822–831.
- Whyte MP 2001 Hypophosphatasia. In: Scriver CR, Beaudet AL, Sly WS, Valle D, Childs B, Kinzler KW, Vogelstein B (eds.) *The Metabolic and Molecular Bases of Inherited Disease*, 8th ed., vol. 4. McGraw-Hill, New York, NY, USA, pp. 5313–5329.
- Weiss M, Cole DEC, Ray K, Whyte M, Lafferty MA, Mullivor RA, Harris H 1988 A missense mutation in the human liver/bone/kidney alkaline phosphatase gene causing a lethal form of hypophosphatasia. *Proc Natl Acad Sci USA* **85**:7666–7669.
- Henthorn PS, Raducha M, Fedde K, Lafferty MA, Whyte MP 1992 Different missense mutations at the tissue-nonspecific alkaline phosphatase gene locus in autosomal recessively inherited forms of mild and severe hypophosphatasia. *Proc Natl Acad Sci USA* **89**:9924–9928.
- Henthorn PS, Whyte MP, 1992 Missense mutations of the tissue-nonspecific alkaline phosphatase gene in hypophosphatasia. *Clin Chem* **38**:2501–2505.
- Greenberg CR, Taylor CLD, Haworth JC, Seargeant LE, Phillips S, Triggs-Raine B, Chodirker BN 1993 A homoallelic Gly317 to Asp mutation in ALPL causes the perinatal (lethal) form of hypophosphatasia in Canadian Mennonites. *Genomics* **17**:215–217.
- Ozono K, Yamagata M, Michigami T, Nakajima S, Sakai N, Cai G, Satomura K, Yasui N, Okada S, Nakayama M 1996 Identification of novel missense mutations (Phe310Leu and Gly439Arg) in a neonatal case of hypophosphatasia. *J Clin Endocrinol Metab* **81**:4458–4461.
- Orimo H, Hayashi Z, Watanabe A, Hirayama T, Shimada T 1994 Novel missense and frameshift mutations in the tissue-nonspecific alkaline phosphatase gene in a Japanese patient with hypophosphatasia. *Hum Mol Genet* **3**:1683–1684.
- Mornet E, Taillandier A, Peyramaure S, Kaper F, Mullaer F, Brenner R, Bussiere P, Froisinger P, Godard J, Le Merrer M, Oury JF, Plauchu H, Puddu P, Rival JM, Superti-Furga A, Touraine RL, Serre JL, Simon-Bouy S 1998 Identification of fifteen novel mutations in the tissue-nonspecific alkaline phosphatase (TNSALP) gene in European patients with severe hypophosphatasia. *Eur J Hum Genet* **6**:308–314.
- Mumm S, Jones J, Finnegan P, Whyte MP 2001 Hypophosphatasia: Molecular diagnosis of Rathbun's original case *J Bone Miner Res* **16**:1724–727.
- Mornet E 2000 Hypophosphatasia: Mutations in the tissue-nonspecific alkaline phosphatase gene *Hum Mutat* **15**:309–315.
- Zurutuza L, Muller F, Gibrat JF, Taillandier A, Simon-Bouy B, Serre JL, Mornet A 1999 Correlations of genotype and phenotype in hypophosphatasia. *Hum Mol Genet* **8**:1039–1046.
- Mornet E, Stura E, Lia-Baldini AS, Stigbrand T, Menez A, Le Du MH 2001 Structural evidences for a functional role of human tissue non specific alkaline phosphatase in bone mineralization. *J Biol Chem* **276**:31171–1178.
- Fukushi-Ire M, Ito M, Amaya Y, Ozawa H, Omura S, Ikehara Y, Oda K 2000 Possible interference between tissue-non spe-

- cific alkaline phosphatase with an Arg⁵⁴ to Cys substitution and a counterpart with an Asp²⁷⁷ to Ala substitution found in a compound heterozygote associated with severe hypophosphatasia. *Biochem J* **348**:633–642.
17. Shibata H, Fukushi M, Igarashi A, Misumi Y, Ikehara Y, Ohashi Y, Oda K 1998 Defective intracellular transport of tissue-nonspecific alkaline phosphatase with an Ala¹⁶² to Thr mutation associated with lethal hypophosphatasia. *J Biochem* **123**:968–977.
 18. Fukushi M, Amizuka N, Hoshi K, Ozawa H, Kumagai H, Omura S, Misumi Y, Ikehara Y, Oda K Intracellular retention and degradation of tissue-nonspecific alkaline phosphatase with a Gly³¹⁷ to Asp substitution associated with lethal hypophosphatasia. *Biochem Biophys Res Commun* **246**:613–618.
 19. Tomic M, Sunvejaric I, Savtchenko ES, Blumenberg M 1990 A rapid and simple method for introducing specific mutations into any position of DNA leaving all other positions unaltered. *Nucleic Acids Res* **18**:1656.
 20. Sanchez R, Sali A 2000 Comparative protein structure modeling. Introduction and practical examples with modeller. *Methods Mol Biol* **143**:97–129.
 21. Le Du MH, Stigbrand T, Taussig MJ, Menez A, Stura EA 2001 Crystal structure of alkaline phosphatase from human placenta at 1.8 Å resolution. Implication for a substrate specificity. *J Biol Chem* **276**:9158–9165.
 22. Bossi M, Hoylaerts MF, Millán JL 1993 Modifications in a flexible surface loop modulate the isozyme-specific properties of mammalian alkaline phosphatases. *J Biol Chem* **288**:25409–25416.
 23. Pizauro JM, Ciancaglini P, Leone FA 1995 Characterization of the phosphatidylinositol-specific phospholipase C-released form of rat osseous plate alkaline phosphatase and its possible significance on endochondral ossification. *Mol Cell Biochem* **152**:121–129.
 24. Heinonen JK, Lahti RJ 1981 A new and convenient colorimetric determination of inorganic orthophosphate and its application to the assay of inorganic pyrophosphatase. *Anal Biochem* **113**:313–317.
 25. Whitby LG, Moss DW 1975 Analysis of heat inactivation curves of alkaline phosphatase isoenzymes in serum. *Clin Chim Acta* **59**:361–367.
 26. Müller HL, Yamazaki M, Mishigami T, Kageyama T, Schönau E, Schneider P, Ozono K 2000 Asp361 Val mutant of alkaline phosphatase found in patients with dominantly inherited hypophosphatasia inhibits the activity of the wild-type enzyme. *J Clin Endocrinol Metab* **85**:743–747.
 27. Hoylaerts MF, Manes T, Millán JL 1997 Mammalian alkaline phosphatases are allosteric enzymes. *J Biol Chem* **272**:22781–22787.
 28. Watanabe H, Hashimoto-Uoshima M, Goseki-Sone M, Orimo H, Ishikawa I 2001 A novel point mutation (C571T) in the tissue-nonspecific alkaline phosphatase gene in a case of adult-type hypophosphatasia. *Oral Dis* **7**:331–335.
 29. Goseki-Sone M, Orimo H, Iimura T, Takagi Y, Watanabe H, Taketa K, Sato S, Mayanagi H, Shimada T, Oida S 1998 Hypophosphatasia: Identification of five novel missense mutations (G507A, G705A, A748G, T1155C, G1320A) in the tissue-nonspecific alkaline phosphatase gene among Japanese patients. *Hum Mutat Suppl* **1**:S263–S267.
 30. Narisawa S, Fröhlander N, Millán JL 1997 Inactivation of two mouse alkaline phosphatase genes and establishment of a mouse model of infantile hypophosphatasia. *Dev Dyn* **208**:432–446.
 31. Waymire KG, Mahuren JD, Jaje JM, Guilarte TR, Coburn SP, MacGregor GR 1995 Mice lacking tissue non-specific alkaline phosphatase die from seizures due to defective metabolism of vitamin B6. *Nat Genet* **11**:45–51.
 32. Narisawa S, Wennberg C, Millán JL 2001 Abnormal vitamin B6 metabolism causes multiple abnormalities, but not impaired bone mineralization in alkaline phosphatase knockout mice *J Pathol* **193**:125–133.
 33. Johnson KA, Hessle L, Wennberg C, Mauro S, Narisawa S, Goding J, Sano K, Millán JL, Terkeltaub R 2000 Tissue-nonspecific alkaline phosphatase (TNAP) and plasma cell membrane glycoprotein-1 (PC-1) act as selective and mutual antagonists of mineralizing activity by murine osteoblasts. *Am J Physiol Regul Integr Physiol* **279**:R1365–R1377.
 34. Fedde KN, Blair L, Silverstein J, Weinstein RS, Waymire K, MacGregor GR, Narisawa S, Millán JL, Whyte MP 1999 Alkaline phosphatase knock-out mice recapitulate the metabolic and skeletal defects of infantile hypophosphatasia. *J Bone Miner Res* **14**:2015–2026.

Address reprint requests to:
 José Luis Millán, Ph.D.
 The Burnham Institute
 10901 North Torrey Pines Road
 La Jolla, CA 92037, USA

Received in original form October 30, 2001; in revised form January 16, 2002; accepted February 6, 2002.